Thermo-hydraulic analysis for SCWR during power-raising phase of startup

CHEN Juan* ZHOU Tao HOU Zhousen CHENG Wanxu

Institute of Nuclear Thermal-Hydraulic Safety and Standardization, North China Electric Power University, Beijing, China, 102206

Abstract The study of thermal characteristics during startup is one of the most important aspects for safety analysis of supercritical water-cooled reactor (SCWR). According to the given sliding pressure mode of SCWR, thermal analysis on temperature-raising phase and power-raising phase of startup are carried out. Considering the radial heterogeneity of power distribution, thermal characteristics for different assemblies during startup are also put forward. The results show that, during temperature-raising phase with core power increased only, the temperature of moderator, coolant and fuel cladding in inner assemblies are increased with little amplitude. During power-raising phase with core power and feed-water flow rate increased, the coolant temperature keeps unchanged, but the moderator temperature is decreased. With a greater variation of power, fuel cladding temperature shows a greater increase. Furthermore, considering the uneven distribution of radial power, thermo-hydraulic characteristics with uneven cladding temperature distribution shows a certain horizontal heterogeneity for different fuel assemblies, which becomes serious as flow rate and power increase. By adjusting flow rate distribution in different fuel assemblies or changing power setting during startup, the cladding temperature difference could be effectively reduced, which provides a certain reference for startup optimization of SCWR.

Key words Supercritical, Sliding pressure, Temperature-raising, Power-raising, Thermo-hydraulic

1 Introduction

The supercritical water-cooled reactor (SCWR) developed in 1989[1,2] has been recommended as one of the Generation IV reactor concepts in the world, and startup thermal analysis has been an important issue to ensure the SCWR safety. For SCWR, two startup modes are used[3,4]: the constant pressure startup mode, in which the reactor starts at supercritical pressure and operates at this pressure constantly with a flash tank and pressure reducing valves; and the sliding pressure startup mode, in which the reactor starts at a sub-critical pressure and operates at continuously changing pressure with a steam-water separator and a drain tank. From the viewpoint of thermo-hydraulic and stability, theoretical analyses on the two startup modes were carried out[5-7], and feasibility studies on the two startup modes were done to analyze and adjust the operation safety of SCWR. However, parameters would vary complicatedly during the startup, which may affect seriously operating characteristics reliability of SCWR startup, hence the need of in-depth researches on thermal characteristics of SCWR startup. In addition, the uneven distribution of power along radial direction of SCWR may affect startup characteristics. Based on the given sliding pressure curve, thermal hydraulic analysis for the temperature phase and power-raising phase of SCWR startup is detailed carried out. Furthermore, the analysis with uneven power distribution in different assemblies is also put forward. It could provide a certain theoretical reference for startup optimization and startup control of SCWR.

Supported by National Basic Research Program of China (No. 2007CB209804), State Key Laboratory of Reactor System Design Technology (No. 2011-153), and the Fundamental Research Funds for the Key Universities (No. 11QX51).

* Corresponding author. *E-mail address:* chenjuan8410@yahoo.com.cn

Received date: 2011-11-16

2 Research object and startup mode

2.1 Research object

The conceptual design of advanced supercritical pressure light water reactor is taken as the research object, which was proposed by Yamhi *et al.* [8,9] of the University of Tokyo in 2005, with a core of 4.2-m height, in which the fuel assemblies were arranged in two zones: an inner zone (73 fuel assemblies) and an external zone (48 fuel assemblies). According to their design, the feed-water flows into top dome through the main feed-water line, where most of it flows downward through external moderator channels, external coolant channels and inner moderator channels into bottom plenum, in flow ratio of 19.7%, 42.2% and 30%, respectively. The residual 8.1% flow from down-comer flew upward through inner fuel channels as coolant. Finally, it flows into the main steam pipe from the core outlet. The flow chart in inner assemblies is shown in Fig.1. It can be seen that, as the method of node dividing is used for channel calculation modeling, each channel is divided into 40 calculation nodes along axial direction, which begins at node 1 and ends at node 40.

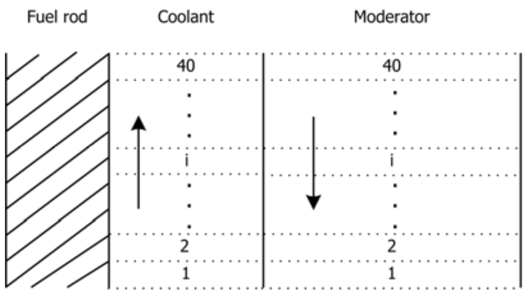

Fig.1 Flow Chart in Inner Assemblies of SCWR.

2.2 Basic parameters

Main parameters for thermo-hydraulic analysis of SCWR during startup are shown in Table 1.

Table 1 Main Parameters of SCWR

Parameters	Design values
Active height/equivalent diameter / m	4.2/3.73
Fuel lattice arrangement	25×25
Number of all fuel assemblies / fuel assemblies of inner assemblies	121/73
Number of fuel rods /water rods per assembly	300/36
Fuel rod outer diameter/ pitch / mm	10.2/11.2
Side length Of square water rods / mm	33.6
Core pressure / MPa	25
Core flow rate under full load operation / $kg{\cdot}s^{-1}$	1262
Coolant inlet/outlet temperature under full load operation / °C	280/500
Average linear power density under full load operation / $kW{\cdot}m^{-1}$	36.68

2.3 Sliding pressure mode

In 2001, the sliding pressure startup mode was proposed by Nakatsuka, *et al.*[6]. Its startup procedure can be differentiated into six phases: starting of nuclear heating at sub-critical pressure, turbine startup, and pressurization to supercritical pressure, switching from startup bypass line to once-through line, temperature-raising phase, and power-raising phase. The sliding pressure curve is shown in Fig.2[6].

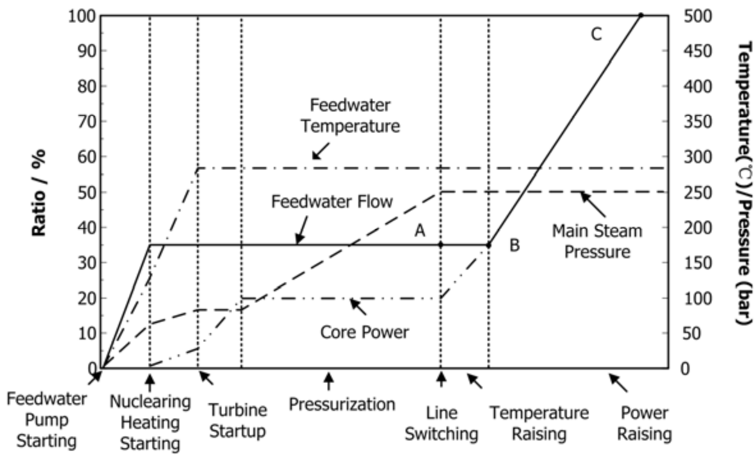

Fig.2 Sliding Pressure Curve of SCWR.

During pressurization phase, core pressure increased from 83 bar (8.3 MPa) to 250 bar (25 MPa). Then the core outlet coolant flow would be usually two phase flow, and the temperature of main steam is equal to the saturated temperature under the sub-critical operating pressure. Thus, it is necessary to provide enough flow to avoid limit-exceeding maximum cladding temperature and prevent it from dry burning during starting especially. Furthermore, no super-heater is designed for supercritical pressure light water reactor, so the core outlet coolant enthalpy must meet the requirement for turbine entry steam enthalpy. Thus, the flow rate should not be too large. According to analyses in references, the minimum flow rate is 35% when the reactor begins to generate heat. The changing scopes of the core power and coolant flow rate in the six startup phases of SCWR are given in Table 2.

Table 2 Changing Scopes of Power and Flowrate in Different Start-up Phases of SCWR

Design parameters	Start of nuclear heating phase	Turbine startup phase	Pressurization phase	Temperature-raising phase	Power-raising phase
Core power	0~5%Q	5%Q~20%Q	20%Q	20%Q~35%Q	35%Q~100%Q
Feed-water Flow rate	35%W	35%W	35%W	35%W	35%W~100%W

*Q is core power and W is feed-water flow rate, in rated operating state

During the stage of temperature-raising and power-raising, there are significantly changes of core power and feed-water flow rate, which may bring obvious influence of startup characteristics. Thus, the following analysis is focusing on these two phases of SCWR startup.

3 Calculation Method

3.1 Neutronics calculation model

3.1.1 Calculation model without radial heterogeneity considered

If the heterogeneity of power distribution along core radial direction was ignored, one-dimensional static physical analysis could be carried out by Eq.(1).

$$Q(\tau) = mn_{\text{fuel}}\sum_{i=0}^{n}(q_{\max}(\tau)f(i)) \qquad (1)$$

where, $Q(\tau)$ is the core power at time τ, W; $q_{\max}(\tau)$ is the maximum linear power density of fuel rods at time τ, W/m; m is the number of assemblies; n_{fuel} is the number of fuel rods in one assemblies; and $f(i)$ is the power factor in node i.

Fig.3 shows the axial power factors used for analysis, calculated by neutronics and thermo-hydraulics coupled method during our previous research[10].

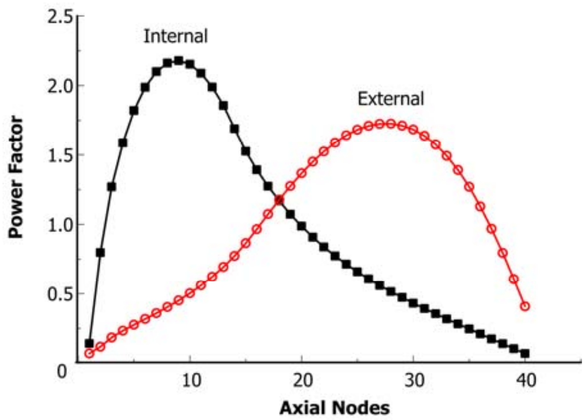

Fig.3 Axial Power Factors of SCWR.

3.1.2 Calculation model with radial heterogeneity distribution considered

Considering the radial heterogeneity distribution, the 2D physical analysis can be done by Eq.(2). The neutron cross section is calculated by the DRAGON code, and power factors of different fuel assemblies are finally obtained by TRIVAC module in DONJON code.

$$Q_i(\tau)=Q(\tau)\varphi(i)/m \qquad (2)$$

where, $Q_i(\tau)$ is the power of i assembly at time τ, W, and $\varphi(i)$ is the power factor of assembly i.

According to the symmetry characteristic of core structure, calculating the power distribution of just 1/8 fuel assemblies can represent the whole core conditions. And the different power factors of the 1/8 fuel assemblies are chosen from the results of our previous work [11]. The numbering and power distribution factor of the 1/8 fuel assemblies are shown in Fig.4.

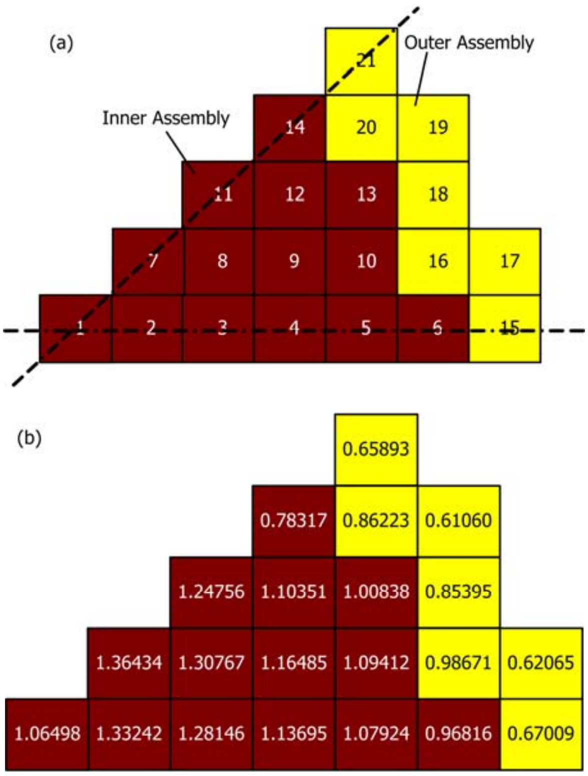

Fig.4 Assemblies numbering (a) and the power factors in the 1/8 core.

3.2 Thermo-hydraulic calculation model

3.2.1 Conservation mathematical model

The model consists of three conservation equations: mass, momentum and energy[12,13], in Eqs.(3−5).

$$\frac{\partial \rho}{\partial \tau}+\frac{\partial(\rho v)}{\partial z}=0 \tag{3}$$

$$\rho\frac{\partial v}{\partial \tau}+\rho v\frac{\partial v}{\partial z}=-\frac{\partial P}{\partial z}\pm\rho g-\frac{f\rho v^2}{2D_e} \tag{4}$$

$$\rho\frac{\partial h}{\partial \tau}+\rho v\frac{\partial h}{\partial z}=q_v^{channel}(\tau) \tag{5}$$

where, z is axial height of one node, m; τ is time, s; ρ is density of coolant or moderator, kg/m^3; v is velocity of coolant or moderator, m/s; P is pressure of coolant or moderator, MPa; h is enthalpy of coolant or moderator, kJ/kg; D_e is equivalent diameter of channels, m; f is friction factor of channels; g is acceleration of gravity, m/s^2; and $q_v^{channel}(\tau)$ is the heat absorbed by coolant or moderator in unit volume at time τ, W/m^3. In addition, + is used for descending flow, and – is used for ascending flow. For coolant, $q_v^{channel}(\tau)$ means the difference of heat absorbed from fuel rods and heat transferred to water rod wall for unit volume coolant; while for moderator, $q_v^{channel}(\tau)$ means the absorbed heat from water rod wall for unit volume moderator.

3.2.2 Heat transfer model between fuel cladding and coolant

The heat transfer between fuel cladding and coolant is calculated by Eq. (6).

$$q_l^{fc} = h_{fc}\ (T_f - T_c) \tag{6}$$

where, q_l^{fc} is the linear power density of fuel rods, W/m; T_f and T_c are the temperature of fuel cladding and coolant, respectively, °C. and h_{fc} is heat transfer coefficient between cladding and coolant, W·m^{-1}·°C^{-1}.

To the SCWR operated at supercritical water conditions, the Watts' correlation [5] is used for convective heat transfer calculation, expressed in Eqs. (7) and (8).

(a) Ascending flow

$$Nu=\begin{cases} Nu_{varp} \\ Nu_{varp}\left(1-\dfrac{3000\overline{Gr_b}}{Re_b^{2.7}\overline{Pr_b}^{0.5}}\right)^{0.295} \\ Nu_{varp}\left(\dfrac{7000\overline{Gr_b}}{Re_b^{2.7}\overline{Pr_b}^{0.5}}\right)^{0.295} \end{cases} \tag{7}$$

For descending flow, the Nusselt number can be calculated by Eq.(8)

$$Nu=Nu_{varp}[1+3000\overline{Gr_b}/(Re_b^{2.7}\overline{Pr_b}^{0.5})]^{0.295} \tag{8}$$

where, $Nu_{varp}=0.021\ Re_b^{0.8}\ \overline{Pr}_b^{0.55}(\rho_w/\rho_b)^{0.35}$; $\overline{Gr_b}=(\rho_b-\overline{\rho})gD_e^3/(\rho_b\mu_b^2)$

$$\overline{Pr_b}=\frac{\overline{C_p}\mu_b}{k_b}$$

$$\overline{\rho}=\frac{\int_{T_b}^{T_p}\rho dT}{T_p-T_b}$$

$$\overline{C_p}=\frac{\int_{T_b}^{T_p}C_p dT}{T_p-T_b}=\frac{h_p-h_b}{T_p-T_b}$$

where, Re_b is Reynolds number of coolant or moderator. $\overline{Pr}_b$, $\overline{Gr}_b$ are Prandtl number and Grashof number respectively; ρ_w and ρ_b are the density of the wall and fluid in flow channels, respectively, kg/m^3; T_p and T_b are temperature of the wall and fluid in flow channels, respectively, °C; h_p and h_b are enthalpy of the wall and fluid in flow channels, respectively, kJ/kg; D_e is equivalent diameter of the fuel channels or moderator channels, m; k_b is heat conductivity of the coolant or moderator, m^{-1}·°C^{-1}; and μ_b is the dynamic viscosity of coolant or moderator, N·s ·m^{-2}.

3.2.3 Heat transfer model between water rod wall and coolant or moderator

The heat transfer from coolant to moderator includes a series of heat transfer process: the convective heat transfer between coolant and water rod wall surface, the conduction of water rods wall, and the convective heat transfer between water rod wall surface and moderator. The calculation model is shown in Eqs.(9) and (10).

$$q_1^{sw} = h_{sw}(T_{sw}-T_w) \tag{9}$$

$$q_1^{sc} = h_{sc}(T_c-T_{sc}) \tag{10}$$

where, q_1^{sw} and q_1^{sc} are the linear power density of inner and outer water pipe walls, respectively, W/m; T_w, T_{sw} and T_{sc} are the temperature of moderator, inner and outer water pipe walls, respectively, °C; h_{sw} is the convective heat transfer coefficients between water pipe inner wall and moderator, and h_{sc} is that between water pipe outer wall and coolant, W·m^{-1}·°C^{-1}. For supercritical pressure, the convective heat transfer coefficient is calculated by Watts' correlation.

3.2.4 Heat conduction model of fuel rods or fuel cladding

The heat conduction for fuel pellet or cladding is calculated by Eq.(11). The fuel pellet is divided into k circular parts along radial direction for detailed analysis.

$$\rho_r c_p{}^r \frac{\partial T_r}{\partial \tau} = \frac{1}{r}\frac{\partial}{\partial r}[k_f(T) r \frac{\partial T_r}{\partial \tau}] + q_v^r \tag{11}$$

where, ρ_r is the density of fuel pellet or fuel cladding, kg·m^{-3}; $c_p{}^r$ is the heat capacity at constant pressure of fuel pellet or fuel cladding, J·kg^{-1}·°C^{-1}; T_r is the temperature of fuel pellet or fuel cladding, °C; k_f is thermal conductivity of fuel pellet or fuel cladding, W·m^{-1}·°C^{-1}; and $q_v{}^r$ is the unit volume heat released, W·m^{-3}.

3.3 Calculating procedure

According to the sliding pressure curve, core power and feed-water flow rate are firstly determined for thermo-hydraulic analysis. Then based on given average linear power density, steady state performance at different time during startup is analyzed by physical and thermo-hydraulic calculation model in Sections 3.1 and 3.2. The calculation procedure is shown in Fig.5.

4 Thermal Characteristics during Startup with Uniform Power Distribution

4.1 Characteristics of moderator temperature

For radial heterogeneity of power distribution is being ignored, the temperature of moderator during the temperature-raising phase is calculated in Eqs.(1), (3) to (11), as well as that during the power-raising phase. Taken typical time as example, the results for the two phases are shown in Fig.6. The moderator temperature decreases from the bottom to the upside by axial direction during startup, mainly because of the descending flow designed for moderator channels of inner assemblies, and reduced opposite heating.

In the temperature-raising phase, the moderator temperature increases with the power, changing from 322.0°C at to 342.2°C at the channel outlet when the power increases from 20% to 35%, mainly due to the increase of core average temperature caused by the core power increase under fixed flow rate of feed-water. As water density decreases and flow velocity increases, so the Reynolds number increases and the Nusselt number increase; whereas the heat capacity at constant pressure decreases, so the Prandtl and Nusselt numbers decrease. As the Reynold number plays a more important role, the Nusselt number finally increases, hence the increase of the heat transfer coefficient and heat flux transferred from coolant to water pipe. With fixed flow rate and channel inlet temperature, moderator temperature increases.

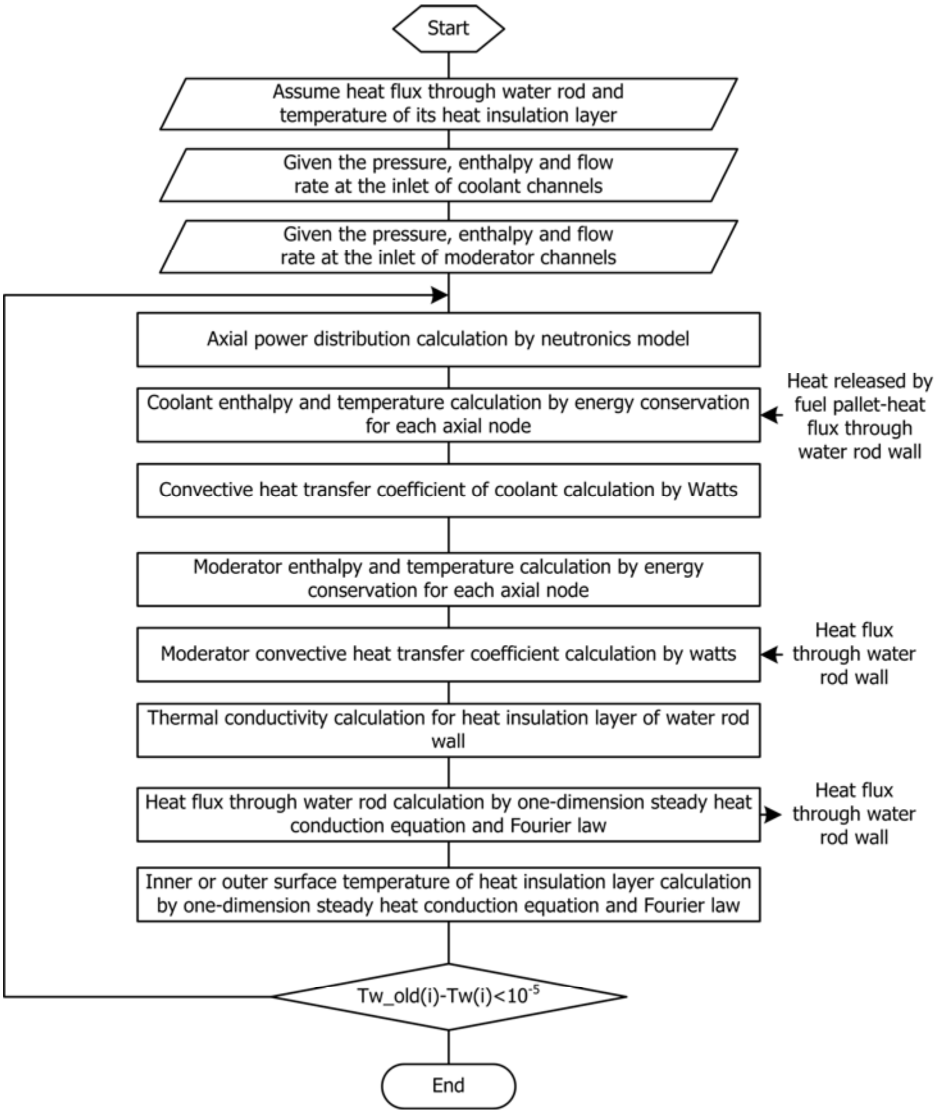

Fig.5 Calculating Procedure for the Thermo-hydraulic Analysis.

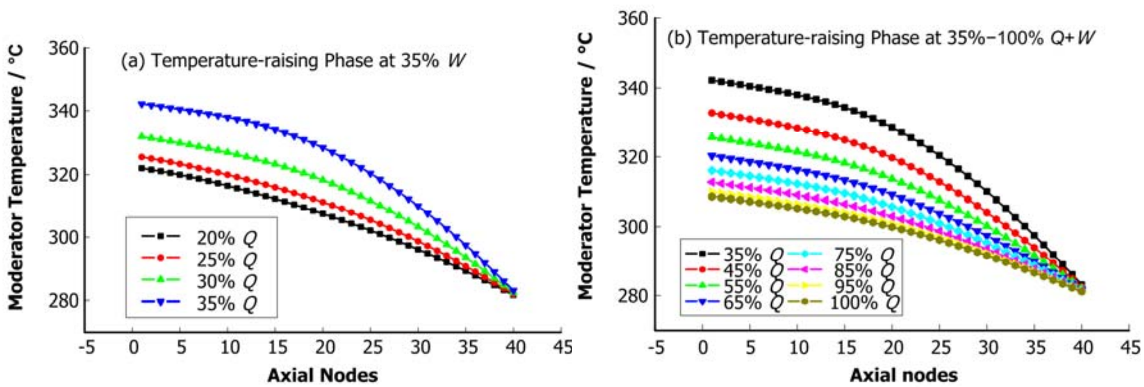

Fig.6 Moderator temperature distribution along axial nodes in typical moments.

Unlike the temperature-raising phase, moderator temperature decreases with increasing power and feed-water flow rate in the power-raising phase. The heat flux through water pipe wall and the moderator temperature increase with the core power under fixed flow rate. With increasing feed-water flow rate, heat absorbed by unit volume moderator, and the moderator temperature, decreases.

In the power-raising phase, with simultaneous increase of the core power and feed-water flow rate, the moderator temperature is reduced as the flow rate effect is dominant even at power/flow-rate ratio=1.

4.2 Characteristics of coolant temperature

With a unifor radial heterogeneity of power distribution, the coolant temperature in the temperature-raising phase, and in the power-raising phase, is calculated by Eq.(1) and Eqs.(3) to (11). The results at typical time are shown in Fig.7, with the coolant temperature for each node. The coolant temperature increases from the bottom to the upside along the axial direction, This is mainly because the upwelling flow is adopted for the fuel channels of inner assemblies, which leads to the heating in the same direction.

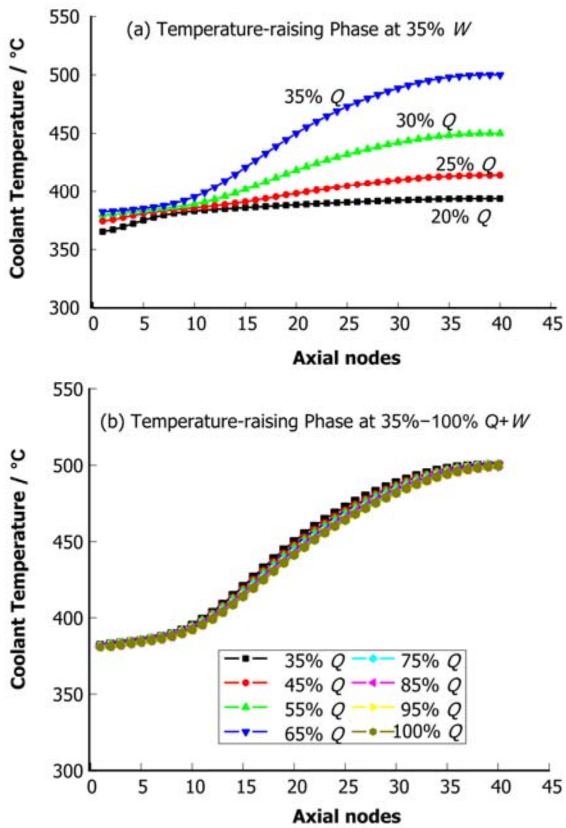

Fig.7 Coolant temperature distribution along axial nodes in different typical time, (a) temperature-raising phase and (b) power-raising Phase.

In the temperature-raising phase, coolant temperature increases with the core power, because of mainly the increase in heat release by fuel rod and heat transferred to coolant. The heat transferred from coolant to outer surface of water pipe increases, in lower amplitude though, but the heat absorbed by coolant increases obviously, hence the coolant temperature increase. The coolant inlet temperature in Fig.6 increases with the moderator temperature. The greater is power increase, the greater increase of coolant temperature.

Changes in amplitude of the axial nodes differ from each other. For example, the core outlet temperature of 106.3°C is much greater than that 8.2°C at the point of 1/3 core height. Because of the continuous rise of coolant temperature from the inlet to the outlet of fuel channels, in a certain location near 1/3 core height, it may well exceed the pseudo-critical point (384°C in 25 MPa), where a peak value of the Prandtl number would appear according to the sudden change of heat capacity at constant pressure. This would cause the convective heat transfer coefficient to increase sharply and decrease immediately. With the same peak of Prandtl number, however, the coolant temperature near this pseudo-critical point at 1/4 core height almost keeps the same.

In the power-raising phase, the core power and coolant flow rate increases, but the coolant temperature keeps unchanged at each axial node, due to the matching increasing pace to the mass flow rate and power.

4.3 Characteristics of maximum cladding temperature

By ignoring radial heterogeneity of power distribution, temperature of fuel cladding surface in the temperature- raising phase, and in the power-raising phase, is calculated by Eqs.(1) and (3) to (11). The results for the two phases at typical time are shown in Fig.8, with the fuel cladding temperature for each node.

From Fig.8, the gradient of fuel cladding temperature from bottom to upside in the axial direction is small in the temperature-raising phase. At any time of the phase, the difference of power among the axial nodes is small under small peak value of the core power, and the heat release is easily conducted by coolant from each axial node, even with higher coolant temperature in the latter periods. Obvious changes can be seen especially near the peak point at 1/3 core height. This is can be attributed to the significant axial power difference under large peak value at 1/4 core height and asymmetric distribution of core power in Fig.3, and to the obvious increase of coolant temperature along the core height. Comparing the curves, the power peak shifts downward in the opposite flow direction, hence the eased cladding temperature increase along the coolant heating direction.

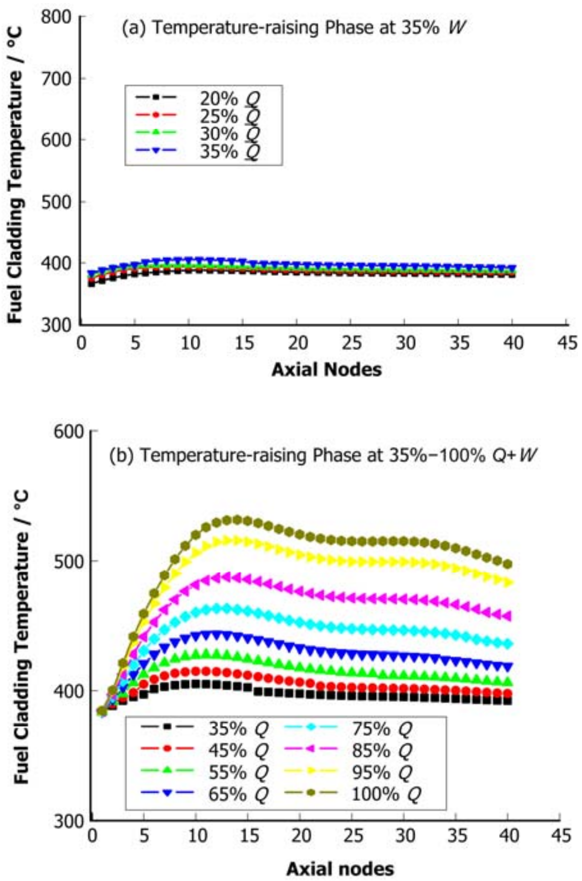

Fig.8 Distribution of fuel cladding temperature along axial nodes at typical moment, (a) Temperature-raising Phase and (b) Power-raising Phase.

In the temperature-raising phase, the maximum cladding temperature increases with the power. In the power- raising phase, the core power and feed-water flow rate increases in the same rate. The maximum cladding temperature increases greatly. For example, with a simultaneous increase from 35% to 100% of the core power and flow rate, the maximum cladding temperature increases from 405.2°C to 531.8°C. The core power increase leads to changes in heat release of the SCWR, and the maximum cladding temperature increases obviously even for the flow rate in the same amplitude at the same time.

A comparative analysis of the power and flow rate effect on the maximum cladding temperature is made. Taking the core power at 50%*Q* and feed-water flow rate at 50%*W*, under calculation conditions of 1) a 15% decrease of the core power and 2) a 15% increase of feed-water flow rate. At the same power and 15% increase of flow rate, the maximum cladding temperature decreases from 421.0°C to 413.8°C; while at the same flow rate and 15% decrease of core power, the maximum cladding temperature even decreases to 399.0°C. So the core power is affects the maximum cladding temperature more significantly, and is an important factor for starting control and startup safety.

5 Thermal characteristics during startup with non-uniform power distribution

5.1 Characteristics of moderator temperature

Considering the radial heterogeneity of power distribution, the temperature of moderator in different assemblies is calculated by Eqs.(2) to (11). The outlet/inlet moderator temperatures for the 1/8 fuel assemblies in three typical times, i.e. the beginning of temperature-raising phase (20%*Q*+35%*W*), the transient phase (35%*Q*+35%*W*), and the ending of power-raising phase (100%*Q*+ 100%*W*) are compared in Fig.9. It can be seen that, in the transient phase, the difference of moderator temperature among the fuel assemblies is the highest of all, with the highest of 375.1°C at No.7 assembly and the lowest of 328.3°C at No.14, i.e. a maximum difference of 46.8°C. At the beginning of temperature-raising phase and ending of power-raising phase, the difference is relative small. Taken the latter as example, as the power and flow rate increase to 100%, No.7 assembly is of the highest temperature of 329.4°C; and No.14 is of the lowest temperature of 301.6°C, with a difference of just 27.8°C.

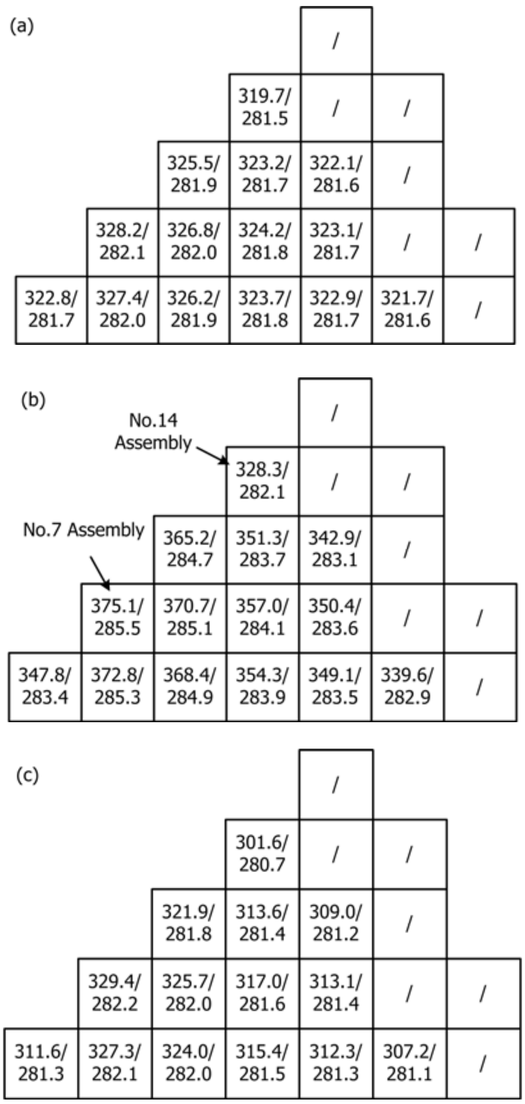

Fig.9 Outlet/inlet moderator temperature of the 1/8 core. (a) 20%*Q*+35%*W*, (b) 35%*Q*+35%*W* and (c) 100%*Q*+100%*W*.

5.2 Characteristics of coolant temperature

Considering the radial heterogeneity of power distribution, the temperature of coolant in different assemblies is calculated by Eqs.(2−11). The outlet/inlet moderator temperatures for the 1/8 fuel assemblies in three typical times, i.e. the beginning of temperature-raising phase (20%*Q*+35%*W*), the transient phase (35%*Q*+35%*W*), and the ending of power-raising phase (100%*Q*+100%*W*) are compared in Fig.10. At the beginning of temperature-raising phase, the coolant temperature in different fuel assemblies differs obviously from each other. For example, the outlet coolant temperature in No.7 fuel assembly is 428.6°C, and the outlet coolant temperature in No.14 fuel assembly is only 386.4°C, with a difference of about 42.2°C. At the transient phase, the coolant temperature difference increases to 241.4°C between No.7 and No.14 assemblies. When the coolant temperature changes a little in the power-raising phase, the coolant temperature distribution changes a little. Compared with Fig.8, the outlet coolant temperature in different assemblies changes differently with the power, increasing from 670.9°C to 701.5°C for No.7 assembly, but decreasing a little (from 429.5°C to 421.6°C) for No.14 assembly. This is mainly because that, with different core power factors of different fuel assemblies, the influence of power and function of flow rate on coolant temperature deviates from their balance for constant coolant temperature.

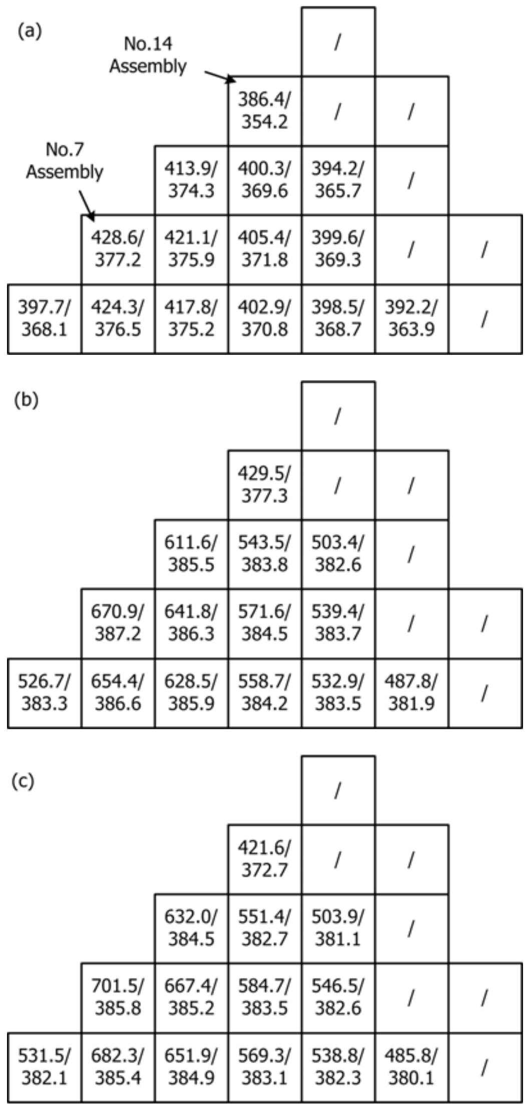

Fig.10 Outlet/inlet coolant temperature of the 1/8 core, (a) 20%*Q*+35%*W*, (b) 35%*Q*+35%*W* and (c) 100%*Q*+100%*W*.

5.3 Characteristics of maximum cladding temperature

Considering the radial heterogeneity of power distribution, the maximum temperature of fuel cladding surface in different assemblies are calculated by Eqs.(2−11). The outlet/inlet moderator temperatures for the 1/8 fuel assemblies in three typical times, i.e. the beginning of temperature-raising phase (20%Q + 35%W), the transient phase (35%Q + 35%W), and the ending of power-raising phase (100%Q + 100%W) are compared in Fig.11. At the ending of power-raising phase, the maximum cladding temperature of fuel assemblies differs with each other, with the highest of 598.8°C No.7 assembly, the lowest of 500.3°C at No.14;assembly, and a difference of 98.5°C between the two assemblies.

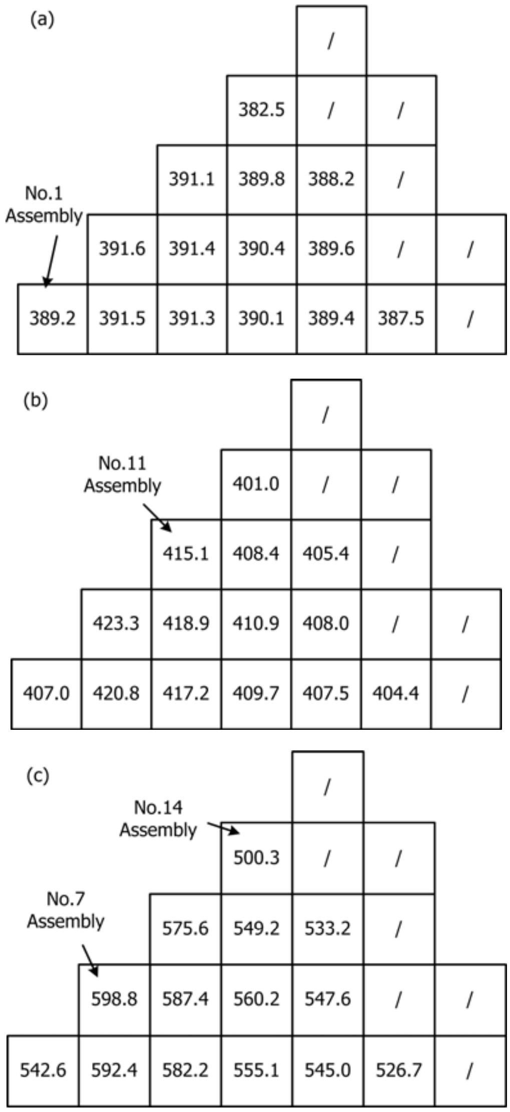

Fig.11 Maximum cladding temperature of the 1/8 core, (a) 20%Q+35%W, (b) 35%Q+35%W and (c)100%Q+100%W.

At the beginning of temperature-raising phase and the transient phase, the maximum cladding temperature of different fuel assemblies differs little from each other. In order to explain the impact of power factor on maximum cladding temperature, finer changes in the two phases are calculated. The results of No.1, No.7, No.11 and No.14 assemblies are given in Fig.12. In the temperature-raising phase, the power factor affects little on the maximum cladding temperature difference, while in the power-raising phase, the difference between different fuel assemblies increases obviously with both power and coolant flow rate, from 9.1°C of No.7 assembly to 98.5°C of No.14 assembly. In this condition, non-uniform distribution of the cladding temperature, and non-uniform thermal characteristics, is obvious in the power-raising phase.

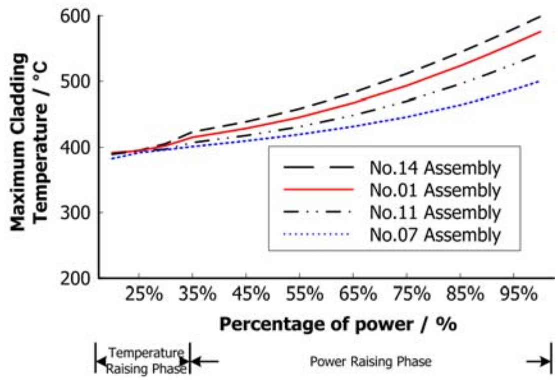

Fig.12 Maximum cladding temperature for typical fuel assemblies

6 Optimization design of slipping startup for supercritical pressure light water reactor

The maximum cladding temperature in consideration of the radial heterogeneity of power distribution is far higher than that without considering the radial heterogeneity of power distribution. Thus, the non-uniform power distribution is a serious challenge to startup safety of supercritical pressure light water reactor, such as the stability of thermal characteristics. In this regard, two schemes are proposed to reduce the degree of non-uniform thermal characteristic in the startup: to adjust flow rate distribution in different fuel assemblies and calculate the flow rate in each fuel assembly with corresponding power factors under fixed flow rate of total coolant in the core; and to change the power rate at different moments, with a

15% reduction—on the basis of pervious startup curve— of the core power rate in each fuel assembly , under fixed total coolant flow rate.

According to the two schemes, the maximum cladding temperature of typical fuel assemblies in the power- raising phase are calculated by Eqs. (2) to (11). The results of No.1, No.7, No.11 and No.14 assemblies, are given in Fig.13, with the coolant flow rate being abscissa to represent the time for convenient comparison, as total coolant flow rate in different assemblies is always equal with each other at any time of the power-raising phase. The difference of the maximum cladding temperature between different fuel assemblies is effectively reduced by either scheme, which solves effectively the space heterogeneity of thermal characteristics. The difference of maximum cladding temperature between No.14 and N0.7 assemblies is about 98.5°C before optimization, while it is 6.9°C with Scheme 1 and 51.7°C with Scheme 2. Thus Scheme 1 is better. Also, Scheme 2 may cause decrease of the maximum temperature for each fuel assembly. Such as N0.7 assembly, the maximum temperature increases to 507.5°C, which is lower than 528.3°C of Scheme 1.

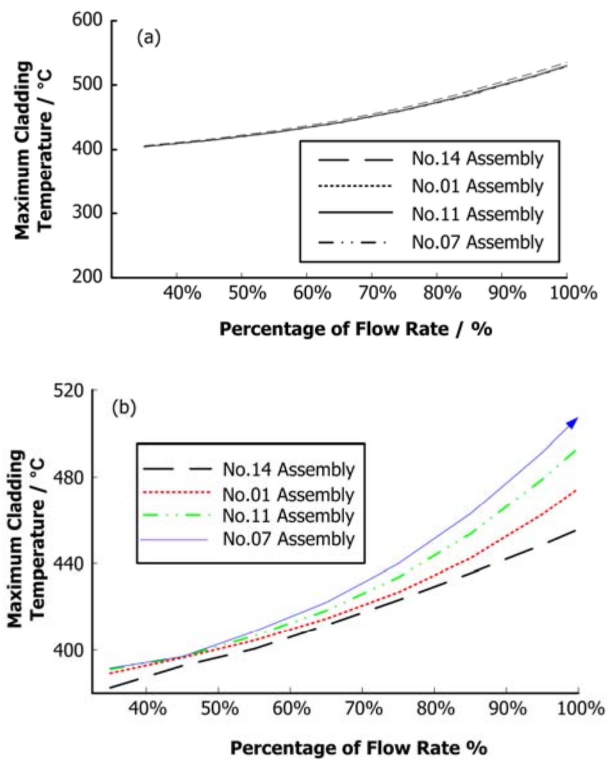

Fig.13 Optimized maximum cladding temperature for typical fuel assemblies.

In the above calculation, the neutron section in rated condition are used for all conditions in the startup, which needs further research considering effects of obvious changes in coolant and moderator temperature.

7 Conclusion

Taking supercritical LWR proposed by Japan as research object, a startup computation code for supercritical water-cooled reactor is developed. Then detailed thermal analysis on temperature-raising phase and power-raising phase of startup are carried out. In which, the thermal characteristics with uneven radial power distribution are further considered in average flow distribution. The results are summarized as follows.

(1) During temperature-raising phase, the maximum cladding temperature is increased with power increased only. But during power-raising phase, when the core power and flow rate increase with the same amplitude, the maximum cladding temperature is increased and with even wilder increasing extent. So the core power is likely to influence the maximum cladding temperature more significantly and it should be one of the most important factors for starting control and startup safety.

(2) During temperature-raising phase, moderator temperature is increased followed with power raised only. And during power-raising phase, when power and flow rate simultaneous increase, the moderator temperature will be decreased as the influence of flow rate occupy a dominant position, which shows the opposite effects.

(3) During temperature-raising phase, coolant temperature in inner fuel assemblies is increased with power increased only. And during power-raising phase, when core power and flow rate are increased, the coolant temperature would keep unchanged at each axial node.

(4) The radial heterogeneity of power distribution has a certain influence on the difference of the maximum cladding temperature, especially for power-raising phase. And the difference between different fuel assemblies will be obviously increased with the power and flow rate, which may lead to even larger uneven level of thermal characteristics. The maximum

cladding temperature difference could be effectively reduced by adjusting the flow rate distribution in different fuel assemblies or reducing the power percentage at different time, which is effective to deal with space heterogeneity of thermal characteristics. Furthermore, to reduce the power percentage at corresponded time of previous startup curve may lead to the decrease of the maximum temperature for each fuel assembly, too.

References

1 Mukohara T, Koshizuka S, Oka Y, *et al*.Ann Nucl Energy, 1999, **16:** 1423–1436.

2 Yamaji A, Kamei K, Oka Y, *et al*. Ann Nucl Energy, 2005, **32:** 651–670.

3 Yi T T, Ishiwatari Y, Koshizuka S, *et al.* J Nucl Sci Technol, 2004, **41:** 790–801.

4 Yi T T, Ishiwatari Y, Liu J, *et al*. J Nucl Sci Technol, 2005, **42:** 537–548.

5 Cai J, Ishiwatari Y, Ikejiri S, *et al*. Nucl Eng Des, 2009, **29:** 665–679.

6 Nakatsuka T, Oka Y, Koshizuka S. Nucl Technol, 2000, **134:** 221–230.

7 Shan J Q, Pan J J, Yang J, *et al*. Nucl Eng Des, 2010, **24:** 1005–1012.

8 Yamaji A, Kamei K, Oka Y, *et al*. Ann Nucl Energy, 2005, **32:** 651–670.

9 Kamei K, Yamaji A, Ishiwatari Y, *et al*. Proc ICAPP'05, Seoul, Korea, 2005.

10 Chen J, Zhou T, Hou Z S, *et al*. Adv Mater Res, 2012, **472-475:** 278–283.

11 Li Z Y. Research on neutronic and thermal-hydraulic programs in supercritical water-cooled reactor, thesis for the master degree, Beijing: North China Electric Power University, 2010, 60–61.

12 Li Z Y, Zhou T, Sun C H, *et al*. 18th International Conf. on Nuclear Engineering, ICONE18-29537, Xi'an, China, 2010.

13 Li Z Y, Zhou T, Sun C H. Nucl Power Eng, 2011, **32:** 52–57.